

Magnetic flux transitions in two-band single-junction superconductors with time-reversal symmetry breaking

Guo Wang(王果), Tian-Yi Han(韩天意), and Hai Huang(黄海)

Citation: Chin. Phys. B, 2025, 34 (**3**): 037401. DOI: 10.1088/1674-1056/ada431
Journal homepage: http://cpb.iphy.ac.cn; http://iopscience.iop.org/cpb

What follows is a list of articles you may be interested in

Pairing correlation of the kagome-lattice Hubbard model with the nearest-neighbor interaction

Chen Yang(杨晨), Chao Chen(陈超), Runyu Ma(马润宇), Ying Liang(梁颖), and Tianxing Ma(马天星)
Chin. Phys. B, 2024, 33 (**10**): 107404. DOI: 10.1088/1674-1056/ad7578

Spin-polarized pairing induced by the magnetic field in the Bernal bilayer graphene

Yan Huang(黄妍) and Tao Zhou(周涛)
Chin. Phys. B, 2024, 33 (**4**): 047403. DOI: 10.1088/1674-1056/ad102f

Multi-band analysis on physical properties of superconducting FeSe films

Jian-Tao Che(车剑韬) and Chen-Xiao Ye(叶晨骁)
Chin. Phys. B, 2023, 32 (**9**): 097401. DOI: 10.1088/1674-1056/acd3e5

Phase-field simulation of superconductor vortex clustering in the vicinity of ferromagnetic domain bifurcations

Hasnain Mehdi Jafri, Jing Wang(王静), Chao Yang(杨超), Jun-Sheng Wang(王俊升), and Hou-Bing Huang(黄厚兵)
Chin. Phys. B, 2020, 29 (**12**): 127402. DOI: 10.1088/1674-1056/abb22c

Generalized Drude model and electromagnetic screening in metals and superconductors

Da Wang(王达)
Chin. Phys. B, 2018, 27 (**5**): 057401. DOI: 10.1088/1674-1056/27/5/057401

Magnetic flux transitions in two-band single-junction superconductors with time-reversal symmetry breaking

Guo Wang(王果)[1], Tian-Yi Han(韩天意)[1], and Hai Huang(黄海)[2,†]

[1] *School of Nuclear Science and Engineering, North China Electric Power University, Beijing* 102206, *China*
[2] *Department of Mathematics and Physics, North China Electric Power University, Beijing* 102206, *China*

(Received 11 October 2024; revised manuscript received 15 December 2024; accepted manuscript online 31 December 2024)

Based on Ginzburg–Landau theory, we investigate the electromagnetic properties of two-band superconductors with broken time-reversal symmetry. We propose an apparatus of a superconducting ring integrated with a microbridge structure to probe the peculiar topological excitations in the chiral system. The phase difference of two order parameters in the superconductor satisfies the double sine-Gordon equation, and a linear relationship between the phase difference at the two ends of the junction and the total magnetic flux in the ring can be obtained. Then with the Josephson current–phase relation, we establish the dependence of the circulating current and magnetic flux on the applied external magnetic field. Our results show that this single-junction system will exhibit the irreversible behaviors and two different types of fractional flux transitions can clearly manifest the time-reversal symmetry breaking in two-component superconductors.

Keywords: two-band superconducting ring, microbridge, double sine-Gordon equation, fractional magnetic flux

PACS: 74.20.De, 74.20.Rp, 74.20.–z

DOI: 10.1088/1674-1056/ada431 **CSTR:** 32038.14.CPB.ada431

1. Introduction

The discovery of the superconducting F-doped LaFeAsO with $T_c \approx 26$ K has raised a boom of the scientific research on iron-based superconductivity.[1] As the second high-temperature superconductor family, the coexistence of superconductivity and magnetism makes the Fe-based compounds of great value in the exploration of microscopic pairing mechanism and spintronic applications.[2–4] One of the highly interesting problems in these materials is to explore multiband structures and exotic states with broken time-reversal symmetry (BTRS). For example, with the analysis of the superconducting gap evolution, an intermediate s+is state in which the relative phase of order parameters on two hole pockets differs from 0 or π might occur in strongly hole-doped $Ba_{1-x}K_xFe_2As_2$.[5] In addition, this simplest BTRS extension of the most abundant s-wave state is also expected to arise in stoichiometric compound LiFeAs and multiband Josephson junction systems.[6,7]

Up to now, there exist three main experimental probes which can directly indicate the presence of spontaneous magnetization in a superconducting system, so as to detect the BTRS state in a superconductor. The first one is the muon-spin relaxation (μSR) instrument, which can carry out the local measurement of extremely small magnetic field in a sample (down to $\sim 10^{-5}$ T).[8–11] A particular advantage of this technique is that the presence of the BTRS state can be measured in both single crystals and polycrystalline samples. The optical Kerr effect is another very sensitive apparatus for detecting the spontaneous field inside a superconductor by means of the polar Kerr angle.[12–16] However, the reliable determination of the BTRS signal with this method generally requires single crystals, rather than polycrystalline samples. Finally, the superconducting quantum interference device (SQUID) can also be used to discover the BTRS superconducting state, and this approach has already been successfully employed to observe a net magnetization in $LaNiC_2$.[17] But based on the symmetry consideration of the order parameters, the homogeneous s+is state is expected to exclude the spontaneous magnetization in the bulk system, the unequivocal determination of the BTRS signature in unconventional superconductors is still a very challenging problem nowadays.

In this paper, we construct a device consisting of a superconducting ring and a microbridge to detect the BTRS signal in two-band superconductors. The microbridge structure is that two relatively large superconducting regions are linked by a narrow bridge, and such a weak link will behave as a Josephson element whenever the dimensions of the bridge linking the two large superconducting regions are smaller than or at least comparable with the temperature dependent coherence length of the bridge. We study the electromagnetic properties of this combination system based on Ginzburg–Landau (GL) theory. With two types of soliton solutions in the ring and the Josephson current–phase relation in the two-band microbridge,[18] we are able to find the simple analytical expressions for the circulating current and the total magnetic flux as functions of

†Corresponding author. E-mail: huanghai@ncepu.edu.cn

© 2025 Chinese Physical Society and IOP Publishing Ltd. All rights, including for text and data mining, AI training, and similar technologies, are reserved.

applied external magnetic field. Our results show that the observation of two different types of fractional flux transitions in this single-junction system will provide direct evidence for the time-reversal symmetry breaking in two-band superconductors.

The paper is organized as follows. The theoretical formalism is presented in Section 2. Then in Section 3, we discuss the electromagnetic properties of a two-band superconducting ring with a microbridge. We provide our results and discussion in Section 4. Finally, Section 5 gives the conclusion of the paper.

2. Theoretical formalism

The GL free energy functional for the s+is superconducting state can be written as[5,19–23]

$$\begin{aligned} F = & \sum_{\mu=1,2}\left[\frac{1}{2m_\mu}\left|\boldsymbol{\Pi}\Psi_\mu\right|^2-\alpha_\mu\left|\Psi_\mu\right|^2+\frac{\beta_\mu}{2}\left|\Psi_\mu\right|^4\right] \\ & +\gamma_1\left[(\Psi_1^*\Psi_2)^2+\text{c.c.}\right] \\ & +\gamma_2\left|\Psi_1\right|^2\left|\Psi_2\right|^2+\gamma_3\left[(\boldsymbol{\Pi}\Psi_1)^*\cdot\boldsymbol{\Pi}\Psi_2+\text{c.c.}\right]+\frac{\boldsymbol{B}^2}{8\pi}. \end{aligned} \tag{1}$$

Here Ψ_μ represents the superconducting order parameter and m_μ is the effective mass for each band. The coefficient α_μ is a function of temperature, while β_μ is independent of temperature. The quartic coupling coefficients γ_1 and γ_2 are positive phenomenological constants, and γ_3 represents the gradient interaction between these two bands. We define the covariant derivative operator $\boldsymbol{\Pi}=(\nabla-2ie\boldsymbol{A})$ with the vector potential $\boldsymbol{A}$ and the magnetic field $\boldsymbol{B}=\nabla\times\boldsymbol{A}$. We already set $\hbar=c=1$.

Based on an orthogonal transformation between Ψ_1 and Ψ_2, we can actually eliminate the gradient coupling γ_3-term. But the price to pay is that a new Josephson interaction $(\Psi_1^*\Psi_2+\text{c.c.})$ has to be introduced into the system. As a result, the GL functional Eq. (1) can be transformed into the equivalent form

$$\begin{aligned} F = & \sum_{\mu=1,2}\left[\frac{1}{2m_\mu}\left|\boldsymbol{\Pi}\Psi_\mu\right|^2-\alpha_\mu\left|\Psi_\mu\right|^2+\frac{\beta_\mu}{2}\left|\Psi_\mu\right|^4\right] \\ & -\gamma(\Psi_1^*\Psi_2+\text{c.c.})+\gamma_1\left[(\Psi_1^*\Psi_2)^2+\text{c.c.}\right] \\ & +\gamma_2\left|\Psi_1\right|^2\left|\Psi_2\right|^2+\frac{\boldsymbol{B}^2}{8\pi}. \end{aligned} \tag{2}$$

As we know, the GL free energy functional in Eq. (1) can be self-consistently obtained from the three-band Eilenberger equations.[22] Due to the equivalence between the free energy functionals in Eqs. (1) and (2), the theoretical model in Eq. (2) can be derived from the quasiclassical Eilenberger theory as well.

As the distance to the boundary is much greater than the magnetic penetration depth, we can take the London limit and treat the modulus of the order parameter $\Psi_\mu=\left|\Psi_\mu\right|\mathrm{e}^{\mathrm{i}\theta_\mu}$ as constant. For simplicity, we also set the magnetic field $\boldsymbol{B}=B\hat{\boldsymbol{z}}$ in the $\hat{\boldsymbol{z}}$-direction and choose a transverse gauge with the vector potential $\boldsymbol{A}=A\hat{\boldsymbol{x}}$. In this circumstance, the GL functional in Eq. (2) for the one-dimensional system can be written as

$$\begin{aligned} F = & \frac{n_1n_2}{m_1n_2+m_2n_1}\left[\frac{1}{2}\left(\frac{\mathrm{d}\varphi}{\mathrm{d}x}\right)^2+V(\varphi)\right] \\ & +\frac{m_1n_2+m_2n_1}{2m_1m_2}\left(\frac{\mathrm{d}\bar{\theta}}{\mathrm{d}x}-2eA\right)^2 \\ & +\sum_{\mu=1,2}\left(-\alpha_\mu n_\mu+\frac{\beta_\mu}{2}n_\mu^2\right)+\gamma_2n_1n_2+\frac{B^2}{8\pi}. \end{aligned} \tag{3}$$

Here we set $n_\mu=\left|\Psi_\mu\right|^2$ and define $\varphi=\theta_2-\theta_1$ and $\bar{\theta}=(1-\kappa)\theta_1+\kappa\theta_2$ with $\kappa=m_1n_2/(m_1n_2+m_2n_1)$. The potential energy takes the form

$$V(\varphi)=\frac{1}{\lambda^2}\left(-\cos\varphi+\eta\cos2\varphi\right) \tag{4}$$

with

$$\begin{aligned} \frac{1}{\lambda^2} &= 2\gamma\left(\sqrt{\frac{n_2}{n_1}}m_1+\sqrt{\frac{n_1}{n_2}}m_2\right), \\ \eta &= 2\lambda^2\gamma_1\left(m_1n_2+m_2n_1\right). \end{aligned} \tag{5}$$

Note that we are free to redefine the sign of the first term in the potential $V(\varphi)$ by shifting the variable $\varphi\to\varphi+\pi$.

By minimizing the free energy with φ, we can get the double sine-Gordon (DSG) equation for the phase difference

$$\frac{\mathrm{d}^2\varphi}{\mathrm{d}x^2}-\frac{1}{\lambda^2}\left(\sin\varphi-2\eta\sin2\varphi\right)=0. \tag{6}$$

It is a natural extension of the sine-Gordon model because it amounts to adding a second term in the Fourier expansion of a periodic function. The topology of DSG potential changes qualitatively with the value of the parameter η, which leads to unconventional ground state and quasiparticle excitation modes. According to Refs. [24,25], only for the case of $\eta>1/4$, we have two degenerate ground states at $\varphi_0=\cos^{-1}(1/4\eta)$ and $2\pi-\varphi_0$ between 0 and 2π as shown in Fig. 1(a). Since the phase difference in either ground state is not located at 0 or π, it tells us that the DSG model will manifestly break the time-reversal symmetry for $\eta>1/4$. Meanwhile, due to different pathways connecting degenerate ground states, i.e., from $-\varphi_0$ to φ_0 and from φ_0 to $2\pi-\varphi_0$, the DSG equation allows for two elementary topological excitations in the system. The solutions of type I and type II solitons (antisolitons) can be explicitly written down as[24,25]

$$\varphi_{\mathrm{I}}(x)=\pm2\tan^{-1}\left[\sqrt{\frac{4\eta+1}{4\eta-1}}\tanh\left(\sqrt{\frac{16\eta^2-1}{16\eta\lambda^2}}x\right)\right], \tag{7}$$

$$\varphi_{\mathrm{II}}(x)=\pi\pm2\tan^{-1}\left[\sqrt{\frac{4\eta-1}{4\eta+1}}\tanh\left(\sqrt{\frac{16\eta^2-1}{16\eta\lambda^2}}x\right)\right], \tag{8}$$

where $(+)$ refers to soliton and $(-)$ to antisoliton. Type I soliton solution describes a topological excitation where the phase difference crosses the secondary maximum of the potential, while type II soliton solution represents an excitation that crosses the global maximum to connect the ground states. As shown in Fig. 1(b), in a broad x range, the phase changes of type I and type II solitons are $2\varphi_0$ and $2\pi - 2\varphi_0$, respectively.

Note that the α_μ, β_μ and γ_2 terms in Eq. (3) are only functions of the amplitude n_μ and independent of the phase difference φ. From the discussion above, we can see that these terms have no effect on the phase excitations of the superconducting order parameters in our problem.

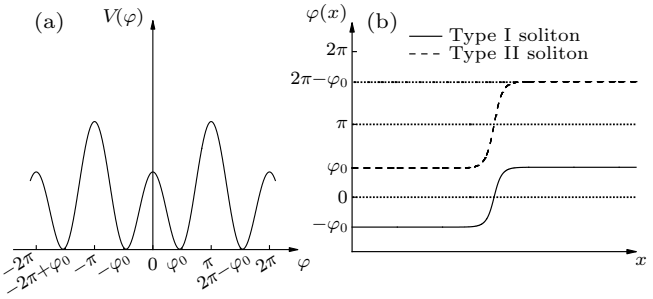


Fig. 1. The schematic illustration of (a) potential energy and (b) two types of soliton excitations in the DSG model for $\eta > 1/4$.

3. Electromagnetic properties of the two-band superconducting ring with a microbridge

Now we discuss a two-band superconducting ring in which a single microbridge is inserted as shown in Fig. 2(a). The geometry of the superconducting microbridge is schematically plotted in Fig. 2(b). The length l and diameter d of the microbridge are assumed to be small as compared to the coherence length of the two-band superconductor. We have the cross section of microbridge $\sigma \propto d^2$.

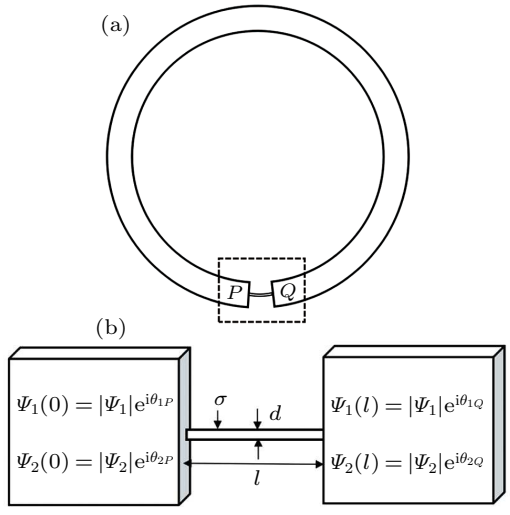


Fig. 2. The schematic illustration of (a) two-band superconducting ring with a microbridge and (b) the geometry of two-band superconducting microbridge.

By minimizing the free energy in Eq. (3) with the vector potential A and combining this formula with the Ampère's law in the Maxwell equations, we can obtain the supercurrent as

$$j = 2e\frac{m_1n_2 + m_2n_1}{m_1m_2}\left(\frac{\mathrm{d}\bar{\theta}}{\mathrm{d}x} - 2eA\right). \tag{9}$$

In the part of the superconducting ring, by integrating the supercurrent in Eq. (9) along the ring, we get

$$\begin{aligned}\int_P^Q j\,\mathrm{d}x \;=\; & 2e\frac{m_1n_2 + m_2n_1}{m_1m_2} \times \Big[(1-\kappa)(\theta_{1Q} - \theta_{1P}) + \\ & \kappa(\theta_{2Q} - \theta_{2P}) - 2\pi\frac{\Phi}{\Phi_0}\Big] \\ =\; & 0\end{aligned} \tag{10}$$

with $\Phi_0 = \pi/e$ the magnetic flux quantum. Here the path of integration is situated at a distance larger than the penetration depth from the ring surface and the supercurrent will vanish in this circumstance. Note that the magnetic flux in the ring is approximated as

$$\Phi \approx \int_P^Q A\,\mathrm{d}x, \tag{11}$$

we then get the following relation from Eq. (10):

$$(1-\kappa)(\theta_{1Q} - \theta_{1P}) + \kappa(\theta_{2Q} - \theta_{2P}) = 2\pi\frac{\Phi}{\Phi_0}, \tag{12}$$

which relates the phase difference across the junction to the magnetic flux in the system.

Now with soliton solutions of the DSG equation in this superconducting structure, we also have

$$\theta_{2Q} - \theta_{1Q} = (\theta_{2P} - \theta_{1P}) + 2\varphi_0N_1 + (2\pi - 2\varphi_0)N_2. \tag{13}$$

Here N_1 and N_2 are integers and denote type I and type II soliton numbers, respectively. Combining this relation with Eq. (12), we can obtain

$$(\theta_{1Q} - \theta_{1P}) + 2\varphi_0\kappa N_1 + (2\pi - 2\varphi_0)\kappa N_2 = 2\pi\frac{\Phi}{\Phi_0}. \tag{14}$$

At this stage, we also note that when an external field is applied, it produces a geometrical flux Φ_e inside the ring and a circulating supercurrent i will be induced which tends to screen the applied flux Φ_e. With the introduction of the inductance of the superconducting ring as L, the total magnetic flux Φ in Eq. (14) is given by

$$\Phi = \Phi_\mathrm{e} - Li. \tag{15}$$

In the part of the microbridge structure, we can solve the one-dimensional GL equations inside the channel with the rigid boundary conditions for the order parameters at both ends.[26] Following Ref. [18], we can neglect all except the gradient terms and solve the equations

$$\frac{\mathrm{d}^2\Psi_1}{\mathrm{d}x^2} = 0 \quad \text{and} \quad \frac{\mathrm{d}^2\Psi_2}{\mathrm{d}x^2} = 0 \tag{16}$$

with the boundary conditions

$$\Psi_1(0)=\sqrt{n_1}\,\mathrm{e}^{\mathrm{i}\theta_{1P}} \quad \text{and} \quad \Psi_1(l)=\sqrt{n_1}\,\mathrm{e}^{\mathrm{i}\theta_{1Q}}, \tag{17}$$

$$\Psi_2(0)=\sqrt{n_2}\,\mathrm{e}^{\mathrm{i}\theta_{2P}} \quad \text{and} \quad \Psi_2(l)=\sqrt{n_2}\,\mathrm{e}^{\mathrm{i}\theta_{2Q}}. \tag{18}$$

Then from the supercurrent expression (5) in Ref. [18], we can obtain the current density in the channel as

$$i=i_1+i_2 \tag{19}$$

with the currents from both bands as

$$i_1=\frac{2e\sigma n_1}{m_1 l}\sin(\theta_{1Q}-\theta_{1P}), \tag{20}$$

$$i_2=\frac{2e\sigma n_2}{m_2 l}\sin(\theta_{2Q}-\theta_{2P}). \tag{21}$$

With Eq. (13), we can rewrite i_2 in Eq. (21) as

$$i_2=\frac{2e\sigma n_2}{m_2 l}\sin\left[\theta_{1Q}-\theta_{1P}+2\varphi_0(N_1-N_2)\right]. \tag{22}$$

Then in the presence of external field, plugging Eqs. (14) and (15) into Eqs. (19)–(22), we get the dimensionless forms of circulating current i and total magnetic flux Φ as

$$\begin{aligned}\frac{Li}{\Phi_0} &= \frac{\beta_\mathrm{e}}{2\pi}\Bigg\{\sin\Bigg[2\pi\left(\frac{\Phi_\mathrm{e}}{\Phi_0}-\frac{Li}{\Phi_0}\right)\\ &\quad -2\varphi_0\kappa N_1-(2\pi-2\varphi_0)\kappa N_2\Bigg]\\ &\quad +\frac{\kappa}{1-\kappa}\sin\Bigg[2\pi\left(\frac{\Phi_\mathrm{e}}{\Phi_0}-\frac{Li}{\Phi_0}\right)-2\varphi_0\kappa N_1\\ &\quad -(2\pi-2\varphi_0)\kappa N_2+2\varphi_0(N_1-N_2)\Bigg]\Bigg\},\end{aligned} \tag{23}$$

$$\begin{aligned}\frac{\Phi_\mathrm{e}}{\Phi_0} &= \frac{\Phi}{\Phi_0}+\frac{\beta_\mathrm{e}}{2\pi}\Bigg\{\sin\left[2\pi\frac{\Phi}{\Phi_0}-2\varphi_0\kappa N_1-(2\pi-2\varphi_0)\kappa N_2\right]\\ &\quad +\frac{\kappa}{1-\kappa}\sin\Bigg[2\pi\frac{\Phi}{\Phi_0}-2\varphi_0\kappa N_1\\ &\quad -(2\pi-2\varphi_0)\kappa N_2+2\varphi_0(N_1-N_2)\Bigg]\Bigg\}\end{aligned} \tag{24}$$

with the definition of $\beta_\mathrm{e}=4\pi e\sigma L n_1/(m_1 l\Phi_0)$. Note that with this framework, we are able to numerically calculate the dependence of circulating current and total magnetic flux on the applied external magnetic field according to Eqs. (23) and (24), respectively. Then we can systematically discuss the fractional flux transitions in this combination system.

4. Results and discussion

In this section, we will set the parameters $\kappa=0.8$, $\varphi_0=\pi/4$ and $\beta_\mathrm{e}=1$ to explore the peculiar magnetic flux transitions in two-band single-junction superconductors with time-reversal symmetry breaking. Since the elementary soliton excitations will be represented by $(N_1,N_2)=(0,0)$, (1, 0) and (0, 1), we will focus on these three branches in our numerical computations.

From Eqs. (23) and (24), we plot the circulating current and the total magnetic flux as functions of external magnetic flux Φ_e in Figs. 3 and 4, respectively. It can be seen that all the curves are multivalued and periodic functions with the period Φ_0. From Figs. 3 and 4, we can see that with the gradual increase of Φ_e, the current and total magnetic flux will first increase along the $(0,0)$ branch to arrive the point A. Then due to the irreversibility, this combination structure will undertake the magnetic flux transition. In this case, the superconducting ring produces a type I soliton and the system will overcome minimum current difference to reach point B on the $(1,0)$ branch as shown in Fig. 3. Then as the external magnetic field continuously increases, the system will sequentially jump from point C on the $(1,0)$ branch to point D on the $(0,1)$ branch and an extra type II soliton can be induced in this process.

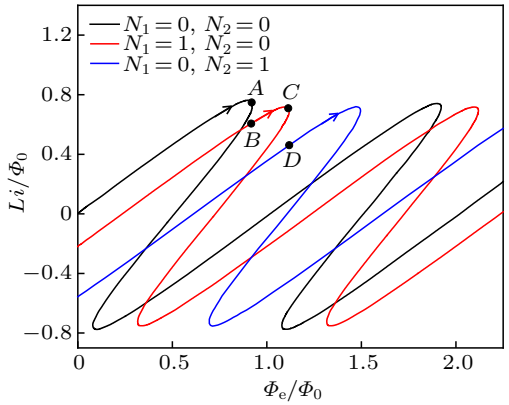


Fig. 3. The dependence of circulating current i on external magnetic flux Φ_e at $\kappa=0.8$, $\varphi_0=\pi/4$ and $\beta_\mathrm{e}=1$.

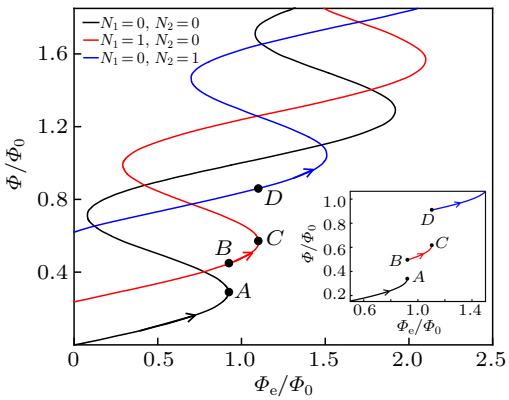


Fig. 4. The dependence of total magnetic flux Φ on external magnetic flux Φ_e at $\kappa=0.8$, $\varphi_0=\pi/4$ and $\beta_\mathrm{e}=1$.

In order to clearly show the peculiar topological excitations in the two-band BTRS superconductor, we also plot the changing curve of total magnetic flux Φ with the gradual increase of Φ_e in the inset of Fig. 4. It can be easily found that there exhibit two types of magnetic flux transitions in the system with flux differences of $0.16\Phi_0$ and $0.32\Phi_0$, respectively. The ratio of these flux transitions is $1/2$, which is consistent with the theoretical estimate of $\varphi_0/(\pi-2\varphi_0)$ with the chosen

parameter $\varphi_0 = \pi/4$. Therefore, two different types of magnetic flux transitions generated in the single-junction system will provide direct evidence for the time-reversal symmetry breaking in the two-band superconductor.

5. Conclusion

In summary, we study the electromagnetic characteristics of superconductors with time-reversal symmetry breaking based on the two-band GL theory. We propose a combination device consisting of a superconducting ring and a microbridge to investigate the distinct topological excitations in the chiral system. With the DSG equation, our numerical calculations give two different types of fractional flux transitions with the increase of external magnetic field, and thus manifest the existence of BTRS superconductivity in this single-junction structure. We hope that our theoretical results will inspire further research on better understanding of the BTRS states and unconventional phase transitions in two-band superconductors.

References

[1] Kamihara Y, Watanabe T, Hirano M and Hosono H 2008 *J. Am. Chem. Soc.* **130** 3296
[2] Mazin I I, Singh D J, Johannes M D and Du M H 2008 *Phys. Rev. Lett.* **101** 057003
[3] Kuroki K, Onari S, Arita R, Usui H, Tanaka Y, Kontani H and Aoki H 2008 *Phys. Rev. Lett.* **101** 087004
[4] Chubukov A V, Efremov D V and Eremin I 2008 *Phys. Rev. B* **78** 134512
[5] Maiti S and Chubukov A V 2013 *Phys. Rev. B* **87** 144511
[6] Ahn F, Eremin I, Knolle J, Zabolotnyy V B, Borisenko S V, Büchner B and Chubukov A V 2014 *Phys. Rev. B* **89** 144513
[7] Ng T K and Nagaosa N 2009 *Europhys. Lett.* **87** 17003
[8] Blundell S J 1999 *Contemp. Phys.* **40** 175
[9] Sonier J E, Brewer J H and Kiefl R F 2000 *Rev. Mod. Phys.* **72** 769
[10] Yaouanc A and de Reotier P D 2011 *Muon Spin Rotation, Relaxation, and Resonance: Applications to Condensed Matter* (Oxford: Oxford University Press)
[11] Khasanov R and Guguchia Z 2015 *Supercond. Sci. Technol.* **28** 034003
[12] Xia J, Maeno Y, Beyersdorf P T, Fejer M M and Kapitulnik A 2006 *Phys. Rev. Lett.* **97** 167002
[13] Schemm E R, Gannon W J, Wishne C M, Halperin W P and Kapitulnik A 2014 *Science* **345** 190
[14] Schemm E R, Baumbach R E, Tobash P H, Ronning F, Bauer E D and Kapitulnik A 2015 *Phys. Rev. B* **91** 140506
[15] Schemm E R, Levenson-Falk E M and Kapitulnik A 2017 *Physica C* **535** 13
[16] Levenson-Falk E M, Schemm E R, Aoki Y, Maple M B and Kapitulnik A 2018 *Phys. Rev. Lett.* **120** 187004
[17] Sumiyama A, Kawakatsu D, Gouchi J, Yamaguchi A, Motoyama G, Hirose Y, Settai R and Onuki Y 2015 *J. Phys. Soc. Jpn.* **84** 013702
[18] Yerin Y S and Omelyanchouk A N 2007 *Low Temp. Phys.* **33** 401
[19] Goncalves W C, Sardella E, Becerra V F, Milošević M V and Peeters F MX 2014 *J. Math. Phys.* **55** 041501
[20] Maiti S, Sigrist M and Chubukov A 2015 *Phys. Rev. B* **91** 161102
[21] Garaud J, Silaev M and Babaev E 2016 *Phys. Rev. Lett.* **116** 097002
[22] Garaud J, Silaev M and Babaev E 2017 *Physica C* **533** 63
[23] Vadimov V L and Silaev M A 2018 *Phys. Rev. B* **98** 104504
[24] Condat C A, Guyer R A and Miller M D 1983 *Phys. Rev. B* **27** 474
[25] Campbell D K, Peyrard M and Sodano P 1986 *Physica D* **19** 165
[26] Kulik I O and Omelyanchouk A N 1976 *Sov. Phys. JETP* **68** 1071